Magnetic anisotropy of single 3*d* spins on a CuN surface

A. B. Shick,[1] F. Máca,[1] and A. I. Lichtenstein[2]
[1]*Institute of Physics ASCR, Na Slovance 2, 18221 Prague 8, Czech Republic*
[2]*University of Hamburg, Jungiusstrasse 9, 20355 Hamburg, Germany*
(Received 23 April 2009; published 21 May 2009)

First-principles calculations of the magnetic anisotropy energy for Mn and Fe atoms on CuN/Cu(001) surface are performed making use of the torque method. The easy magnetization direction is found to be different for Mn and Fe atoms in accord with the experiment. It is shown that the magnetic anisotropy has a single-ion character and mainly originates from the local magnetic moment of Mn and Fe atoms. The uniaxial magnetic anisotropy constants are calculated in reasonable agreement with the experiment.

DOI: 10.1103/PhysRevB.79.172409 PACS number(s): 75.30.Gw, 75.75.+a

Recent scanning tunneling microscopy (STM) measurements of the spin-excitation energies in a magnetic field[1] for individual Fe and Mn atoms on CuN/Cu(001)-$c(2\times2)$ substrate report large values of the axial and transverse magnetic anisotropy energies (MAE) for a single magnetic atom. The STM experiments are complemented by density-functional theoretical calculations. These calculations reveal that the magnetic atoms become incorporated into a covalent CuN matrix so that their electronic and magnetic characters differ from the gas-phase transition-metal atoms. The calculations[1] were performed without spin-orbit coupling (SOC) and did not include the MAE investigation.

These STM experiments[1] along with previously reported x-ray magnetic circular dichroism (XMCD) measurements[2] for a single Co atom and small Co clusters on the Pt(111) surface show that just a few atom-size nanostructures can maintain a stable magnetic orientation at low temperature due to the large magnetic anisotropy energy. What makes these atomic-scale magnetic structures technologically relevant is their large MAE which provides the means of reducing the size of the magnetic bits above the superparamagnetic limit, i.e., the ratio of the MAE to the thermal energy k_BT. Understanding of the atomic-scale MAE in nanomagnets is essential in the determination of the minimum feasible magnetic memory bit size and can assist in further increase in the magnetic recording density.

In the work reported here we make use of *ab initio* numerical calculations of the MAE to analyze the key physical quantities determining the anisotropic magnetic characteristics of single 3*d*-metal atoms on CuN/Cu(001)-$c(2\times2)$ substrate. Similar to the theory of Ref. 1, we use a supercell model. The supercell consists of three Cu(001) layers and a single Cu_2N atomic layer with $c(2\times2)$N-Cu(001) arrangement given in Ref. 3. The in-plane two-dimensional unit cell is doubled (Cu_4N_2) and the 3*d* atom (Mn and Fe) is placed on the top of Cu atom. The supercell is shown schematically in Fig. 1. The vacuum is modeled by the equivalent of four empty Cu layers.

The structure relaxation is performed employing the standard VASP method[4] without SOC and making use of the generalized gradient approximation. Placing 3*d* atom on the top of the Cu atom in the CuN surface makes a substantial rearrangement of the atomic structure (see Fig. 1). The Cu atom right below the adatom moves toward the bulk and the relaxed distance between this atom and magnetic atom is decreasing from 4.42 bohr for the Mn atom to 4.27 bohr for the Fe atom. Other Cu atoms in the CuN top layer change slightly their positions with the change in the magnetic atom. Overall relaxed atomic positions are qualitatively consistent with the picture given in Ref. 1.

We investigate the relativistic electronic and magnetic character of 3*d* atoms on the $c(2\times2)$N-Cu(001) surface. We use the relativistic version of the full-potential-linearized augmented plane-wave method (FP-LAPW) (Ref. 5) in which SOC is included in a self-consistent second-variational procedure.[6] The conventional (von Barth-Hedin) local spin-density approximation (LSDA) is adopted in the calculations, which is expected to be valid for itinerant metallic systems.

The spin M_S and orbital M_L magnetic moments for the magnetization directed along the z axis are given in Table I for the Mn and Fe atoms. Small spin and orbital moments are also induced on neighboring Cu sites and quickly decay away from the magnetic Mn or Fe atom. The spin-resolved projected density of states (PDOS) for the Mn and Fe atoms

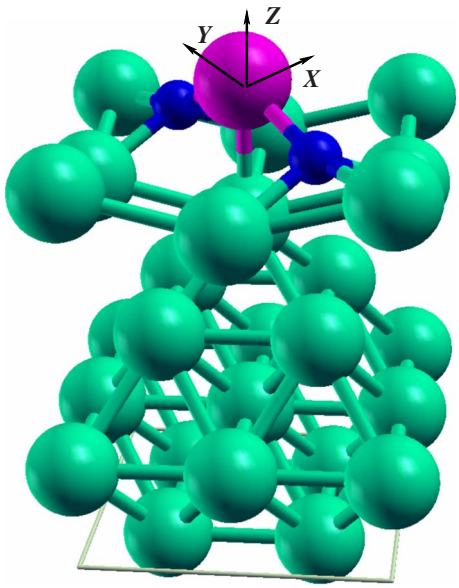

FIG. 1. (Color online) A schematic crystal structure used to represent the 3*d* atom on the $c(2\times2)$N-Cu(001) surface. The actual atomic positions correspond to the case of the Mn atom on the $c(2\times2)$N-Cu(001) surface.

TABLE I. Total spin moment per unit cell (M_S^{Tot}), spin (M_S) and orbital (M_L) magnetic moments on $3d$ adatom (in Bohr magnetons) for the magnetization directed along the z axis.

Atom	M_S^{Tot}	M_S	M_L
Mn	4.379	3.758	0.004
Fe	3.654	2.917	0.076

is shown in Fig. 2. The spin-majority manifold is practically fully occupied for both Mn and Fe. For Mn atom, the spin-minority channel is almost empty and the orbital M_L moment is almost zero. The spin-minority occupation is increased for the Fe adatom while the spin splitting and spin moment M_S are decreasing. The detailed inspection of m_l-projected PDOS shows that nonzero orbital M_L moment for the Fe atom originates from $|m_s=-\frac{1}{2};\ m_l=\pm 2\rangle$ orbitals near Fermi edge. The major contribution to M_L is brought about mainly by in-plane xy and x^2-y^2 spin-minority orbitals. The $3z^2-r^2(\sim|m_l=0\rangle)$ spin-minority orbital (see Fig. 2) does not contribute to M_L. This out-of-plane $3z^2-r^2$ orbital is the least localized due to the strong overlap with $3d$ electrons of the Cu atom beneath.

Next we turn to a salient aspect of our investigation, the MAE calculations. The anisotropic energy $E_A(\theta,\phi)$ dependence (including the second-order terms) on the magnetization direction reads

$$E_A(\theta,\phi) = K_2^{\perp}\mathbf{e}_z^2 + K_2^{\parallel}(\mathbf{e}_x^2 - \mathbf{e}_y^2),$$

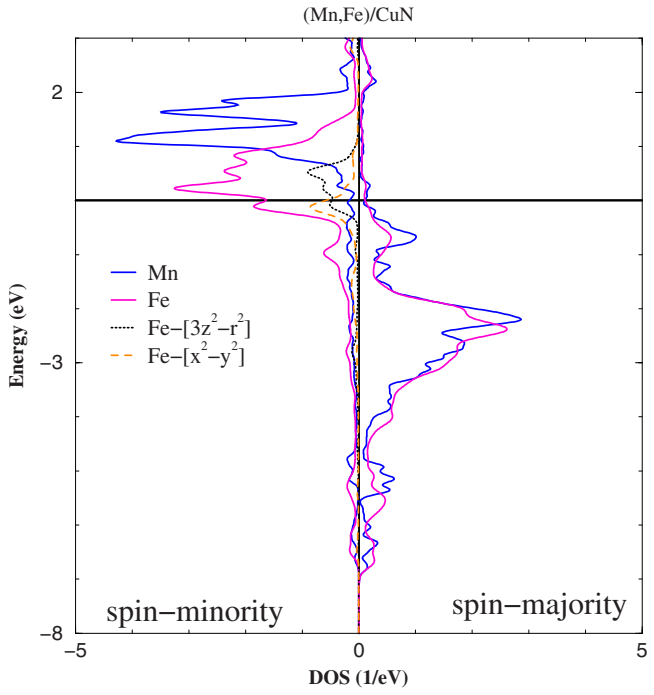

FIG. 2. (Color online) Spin-resolved PDOS for Mn and Fe adatoms. Also shown PDOS for the Fe atom x^2-y^2 and $3z^2-r^2$ spin-minority orbitals.

$$E_A(\theta,\phi) = K_2^{\perp}\cos^2(\theta) + K_2^{\parallel}\sin^2(\theta)[\cos^2(\phi) - \sin^2(\phi)], \tag{1}$$

where $K_2^{\perp}$ and $K_2^{\parallel}$ are the uniaxial MAE constants and $e_{x,y,z}$ are the Cartesian coordinates of the normalized magnetization vector $\vec{\mathbf{M}}/|\vec{\mathbf{M}}|$. The θ and ϕ are the polar angles in the reference frame which is chosen as follows: the x axis is along the in-plane hollow direction, the y axis is along the in-plane N-chain direction, and z axis is along the out-of-plane direction (see Fig. 1).

In order to evaluate the MAE from Eq. (1), we make use of the torque method.[7] It can be formulated as follows. We solve the Kohn-Sham equations for a two-component spinor $|\Phi_i\rangle=\binom{\Phi_i^{\uparrow}}{\Phi_i^{\downarrow}}$ (Ref. 8)

$$\sum_{\beta}[-\nabla^2 + \hat{V}_{\mathrm{eff}} + \xi(\vec{\mathbf{l}}\cdot\vec{\mathbf{s}})]_{\alpha,\beta}\Phi_i^{\beta}(\mathbf{r}) = \epsilon_i\Phi_i^{\alpha}(\mathbf{r}), \tag{2}$$

where the $\hat{V}_{\mathrm{eff}}=V(\mathbf{r})\hat{I}+\boldsymbol{\sigma}\cdot\mathbf{B}(\mathbf{r})$ matrix consists of the sum of the scalar potential V and "exchange" field B parallel to the spin moment M_S, and $\hat{H}_{\mathrm{SO}}=\xi(\vec{\mathbf{l}}\cdot\vec{\mathbf{s}})$ is the spin-orbit (SO) coupling operator. When the magnetic force theorem[9] is used to evaluate the magnetocrystalline anisotropy energy, the M_S is rotated and a single energy-band calculation is performed for the new orientation of M_S. The MAE results from SO coupling induced changes in the band eigenvalues $E_A(\theta,\phi)=\Sigma_i^{\mathrm{occ}}\epsilon_i(\theta,\phi)$. Alternatively, the torque $T(\theta,\phi)=\partial E_A(\theta,\phi)/\partial\theta$ can be evaluated making use of the linear-response theory

$$T(\theta,\phi) = \sum_i^{\mathrm{occ}}\langle\Phi_i'|\frac{\partial\mathbf{U}}{\partial\theta}\xi(\vec{\mathbf{l}}\cdot\vec{\mathbf{s}})\mathbf{U}^{\dagger} + \mathbf{U}\xi(\vec{\mathbf{l}}\cdot\vec{\mathbf{s}})\frac{\partial\mathbf{U}^{\dagger}}{\partial\theta}|\Phi_i'\rangle, \tag{3}$$

where the $\mathbf{U}(\theta,\phi)$ is a conventional spin-rotation matrix and $|\Phi'\rangle=\mathbf{U}(\theta,\phi)|\Phi\rangle$. An advantage of this approach is that it allows the total MAE separation into the element-specific contributions from different atoms in the unit cell. The torque method has been first implemented in FP-LAPW basis in Ref. 10. Also, it has been employed recently in the Korringa-Kohn-Rostocker calculations.[11]

The torque $T(\theta,\phi)$ angular dependence is shown in Fig. 3 for both Mn and Fe atoms on CuN/Cu(001). A set of 784 k points in the full two-dimensional Brillouin zone (2D BZ), which is equivalent to 3136 k points in the full 2D BZ of Cu(001), is used in these calculations. The uniaxial MAE constants $K_2^{\perp}$ and $K_2^{\parallel}$ can be evaluated from the torque $T(\theta,\phi)$ angular dependence, shown in Fig. 3 and angular derivative of Eq. (1),

$$T(\theta,\phi) = [-K_2^{\perp} + K_2^{\parallel}\cos(2\phi)]\sin(2\theta). \tag{4}$$

For the Mn atom, the values of the uniaxial MAE constants are $K_2^{\perp}=-0.20$ meV and $K_2^{\parallel}=-0.17$ meV. The Mn atom contribution in $K_2^{\perp}=-0.16$ meV and $K_2^{\parallel}=-0.12$ meV. For the Fe atom, $K_2^{\perp}=0.16$ meV and $K_2^{\parallel}=0.93$ meV, and the Fe atom specific contributions in $K_2^{\perp}=-0.04$ meV and $K_2^{\parallel}=0.97$ meV. Also, we found that higher-order anisotropy is much less (at least by an order of magnitude) than the uniaxial anisotropy.

Now we evaluate the MAE defined as the energy $E_A(\theta,\phi)$

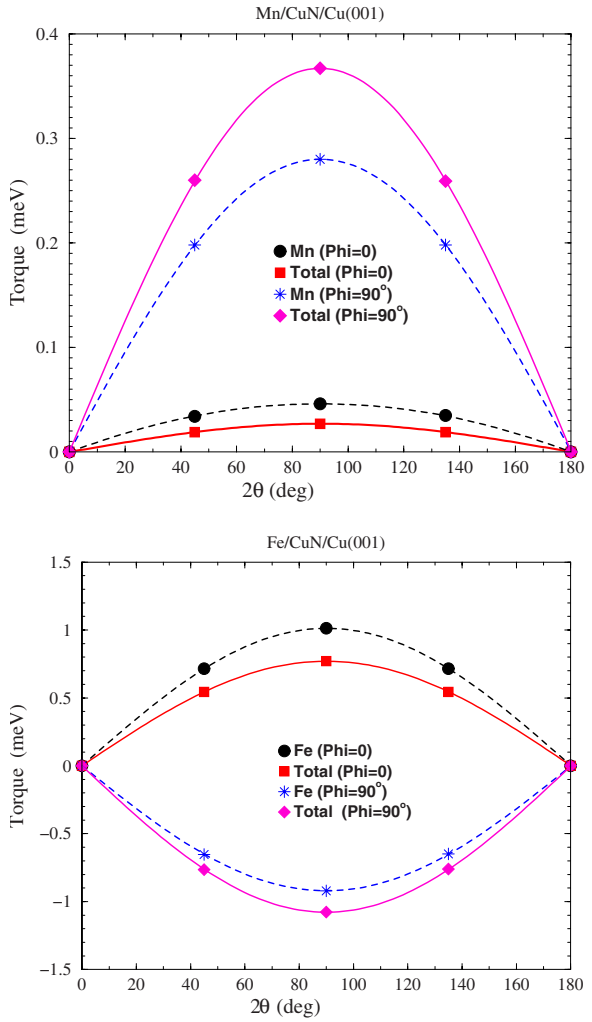

FIG. 3. (Color online) The torque $T(\theta,\phi)$ for the x-z plane (ϕ=0°) and y-z plane (ϕ=90°) as a function of θ. The total torque and leading contributions from the 3d adatom are shown.

difference for different directions of the magnetization M. Using the torque $T(\theta,\phi)$ angular dependence shown in Fig. 3, we obtain MAE=$\int_0^{\pi/2} d\theta T(\theta,\phi)$. The values of the MAE are shown in Table II. There is an increase in the MAE from Mn to the Fe atom case. For the Mn atom, the easy magnetization axis is directed along the surface-normal z axis in agreement with the experimental data.[1] For the case of Fe, the easy magnetization is along the N chain, also in agreement with the experiment.[1] The anisotropic energy $E_A(\theta,\phi)$ angular dependence for Mn and Fe atoms on CuN surface together with the easy magnetization axis orientation is illustrated in Fig. 4.

TABLE II. The MAE (meV) for the Mn and Fe adatoms. Here, $\Delta E[i-j]=E_A[M\|j]-E_A[M\|i]$ and $i(j)=x,y,z$.

Total MAE	Mn	Fe
$\Delta E_A[z-x]$	−0.03	−0.77
$\Delta E_A[z-y]$	−0.37	1.08
$\Delta E_A[y-x]$	0.34	−1.86

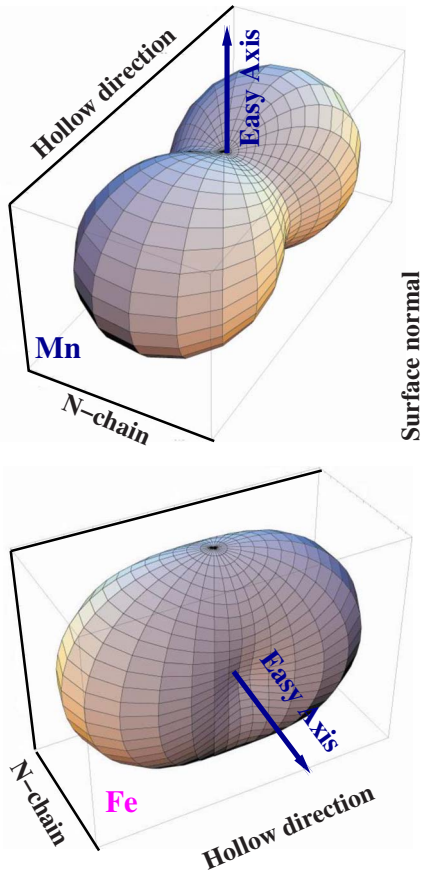

FIG. 4. (Color online) The anisotropic energy $\{\theta,\phi\}$ angular dependence for Mn (top) and Fe (bottom) atoms on CuN surface. Here the length of radius vector forming the surface is equal to $[E_A(\theta,\phi)-E_A(\text{easy axis})]$.

It is quite common to examine the correlation between the MAE and the orbital moment anisotropy (OMA). Approximate relation between the MAE and OMA is given by Bruno formula,[12] [MAE$\approx -\xi/4$OMA], where ξ is the SOC constant. For the Mn atom case, the Bruno formula gives $\Delta E_A[z-x]$ of −0.07 meV, $\Delta E_A[z-y]$ of −0.02 meV, and $\Delta E_A[y-x]$ of −0.05 meV. Comparison with the torque results of Table II shows that Bruno formula yields the correct easy z axis but fails to describe the y-x-plane transverse anisotropy. For the case of Fe atom, making use of Bruno formula we obtain the MAE of $\Delta E_A[z-x]=-0.74$ meV, $\Delta E_A[z-y]=1.46$ meV, and $\Delta E_A[y-x]=-2.19$ meV in a good agreement with the torque results (see Table II). The reason why Bruno formula works better for Fe atom than for Mn atom case is that it is not accurate enough to account for relatively small Mn atom MAE. For the stronger Fe atom MAE, validity of Bruno formula is improving on qualitative.

Now we turn to the comparison with the experimental results of Hirjibehedin *et al.*[1] The STM measures the spin-excitation energies in a magnetic field. These excitation spectra are then analyzed by the model Hamiltonian

$$\hat{H} = g\mu_B \mathbf{BS} + D\mathbf{S}_z^2 + E(\mathbf{S}_x^2 - \mathbf{S}_y^2). \quad (5)$$

In Eq. (5), the z axis is chosen along the easy magnetization direction. In order to compare our results with the experi-

TABLE III. Comparison with experimental D and E (meV). Here, for the Mn atom case, the x axis is along N chain, the y axis is along the hollow direction, and the z axis is out of plane. For the Fe atom case, the x axis is along the hollow direction, the y axis is out of plane, and the z axis along N chain (Ref. 1).

Mn	D (meV)	E (meV)
Exp.	-0.039 ± 0.001	0.007 ± 0.001
LSDA	-0.03	0.03
Fe	D (meV)	E (meV)
Exp.	-1.55 ± 0.01	0.31 ± 0.01
LSDA	-0.36	0.10

ment, we have to convert the data in Table II into the reference frame chosen in Ref. 1 and renormalize the anisotropy values by S^2 ($S=\frac{5}{2}$ for Mn and $S=2$ for Fe). The results are shown in Table III. Our *ab initio* results correctly reproduce the sign and order of magnitude of D and E experimental anisotropies.

It is quite surprising that the LSDA-based calculations give quite reasonable values of the MAE constants for the systems which have been initially thought as being close to the atomic limit. The density-functional theory is known to work reasonably well for the ground-state energy determination and the MAE is defined as the constrained ground-state energy difference for different magnetization directions. Most probably, that is why the MAE results of density-functional theory resemble the values of the uniaxial MAE constants experimentally determined from the spin-excitation spectra of the atomic spin. On the other hand, the electron correlation effects beyond those which are already included in LSDA can play an essential role in more accurate theoretical modeling and interpretation of the experimental data.[1]

Further progress in realistic calculations of the ground-state properties and excitations for single atomic spin on the surface will be made on the basis of the newly emerging combination of the LSDA and dynamical mean-field theory.[13] The electron correlations can modify the electronic structure and produce additional orbital polarization (OP). We estimate the OP effect for the Fe atom with the aim of static mean-field LSDA+U method[14] and find the Fe atom $M_L=0.14\ \mu_B$ to increase by a factor of 2 from its LSDA value of 0.08 μ_B (see Table I). Similar OP-induced increase is expected for the Fe-MAE constants from Table III.

In conclusion, we have shown that the magnetic anisotropy energies for Mn and Fe atoms on CuN/Cu(001) can be semiqualitatively reproduced by the first-principles LSDA FP-LAPW calculations. The easy magnetization direction is found in agreement with the experimental data for Mn and Fe atoms. It is shown that the calculated MAE has a single-ion character and mainly originates from the well-localized moment of Mn and Fe atoms. The uniaxial MAE constants are calculated in semiquantitative agreement with the experiment.

We gratefully acknowledge discussions with K. von Bergmann, H. Brune, and P. M. Oppeneer. Financial support was provided by the Grant Agency of the Academy of Sciences under Project No. IAA100100912, DFG under Grant No. SFB668-A3 (Germany), and German-Czech collaboration program under Projects No. 436TSE113/53/0-1 and No. GACR 202/07/J047.

[1] C. F. Hirjibehedin, C.-Y. Lin, A. F. Otte, M. Ternes, C. P. Lutz, B. A. Jones, and A. J. Heinrich, Science **317**, 1199 (2007).
[2] P. Gambardella, S. Rusponi, M. Veronese, S. S. Dhesi, C. Grazioli, A. Dallmeyer, I. Cabria, R. Zeller, P. H. Dederichs, K. Kern, C. Carbone, and H. Brune, Science **300**, 1130 (2003).
[3] Y. Yoshimoto and S. Tsuneyuki, Surf. Sci. **514**, 200 (2002).
[4] G. Kresse and J. Hafner, Phys. Rev. B **47**, 558 (1993); G. Kresse and J. Furthmüller, Comput. Mater. Sci. **6**, 15 (1996); G. Kresse and D. Joubert, Phys. Rev. B **59**, 1758 (1999).
[5] D. J. Singh, *Planewaves, Pseudopotentials and the LAPW Method* (Kluwer, Boston, 1994), p. 115.
[6] A. B. Shick, D. L. Novikov, and A. J. Freeman, Phys. Rev. B **56**, R14259 (1997).
[7] S. A. Turzhevskii, A. I. Likhtenstein, and M. I. Katsnelson, Sov. Phys. Solid State **32**, 1952 (1990).
[8] To simplify the notation, we use Pauli-type Hamiltonian including SOC while the actual implementation contains in addition the scalar-relativistic terms.
[9] A. I. Liechtenstein, M. I. Katsnelson, V. P. Antropov, and V. A. Gubanov, J. Magn. Magn. Mater. **67**, 65 (1987); M. Methfessel and J. Kubler, J. Phys. F **12**, 141 (1982).
[10] X. Wang, R. Wu, D.-S. Wang, and A. J. Freeman, Phys. Rev. B **54**, 61 (1996).
[11] J. B. Staunton, L. Szunyogh, A. Buruzs, B. L. Gyorffy, S. Ostanin, and L. Udvardi, Phys. Rev. B **74**, 144411 (2006).
[12] P. Bruno, Phys. Rev. B **39**, 865 (1989).
[13] A. Georges, G. Kotliar, W. Krauth, and M. Rozenberg, Rev. Mod. Phys. **68**, 13 (1996).
[14] A. B. Shick and W. E. Pickett, Phys. Rev. Lett. **86**, 300 (2001) and references therein. In these calculations, Coulomb $U=2$ eV and exchange $J=0.84$ eV were used.